Inorg. Chem. **2005**, *44*, 8916–8928

Complexation to Fe^{II}, Ni^{II}, and Zn^{II} of Multidentate Ligands Resulting from Condensation of 2-Pyridinecarboxaldehyde with α,ω-Triamines: Selective Imidazolidine/Hexahydropyrimidine Ring Opening Revisited

Nicolas Bréfuel, Christine Lepetit, Sergiu Shova,† Françoise Dahan, and Jean-Pierre Tuchagues*

Laboratoire de Chimie de Coordination du CNRS, UPR 8241, 205 route de Narbonne, 31077 Toulouse Cedex, France

Received May 17, 2005

The condensation reaction between 2-pyridinecarboxaldehyde and diethylenetriamine, 3-[(2-aminoethyl)amino]-propylamine, and 3,3′-iminobis(propylamine) in a 2:1 molar ratio yields ligands that may be isolated exclusively in the dissymmetric (cyclic) isomeric forms L^A, L^B/L^{B*}, and L^C. The template effect of a metal center (Fe^{II}, Ni^{II},and Zn^{II}) results in the ring opening of L^C including one hexahydropyrimidine ring and one (long) propylene bridge. The resulting symmetric bis-Schiff base isomeric form $L^{C'}$ is stabilized through pentacoordination, yielding $[Fe^{II}L^{C'}(NCS)](NCS)$ (**3**), $[Ni^{II}L^{C'}(NCS)](NCS)$ (**6**), and $[Zn^{II}L^{C'}(NCS)](NCS)$ (**9**). The same metal centers are too bulky to exert a template effect on L^A including one imidazolidine ring and one (short) ethylene bridge. L^A acts as a tetradentate ligand yielding $[Fe^{II}L^A(NCS)_2]$ (**1**), $[Ni^{II}L^A(NCS)_2]$ (**4**), and $[Zn^{II}L^A(NCS)_2]$ (**7**). The template effect of the metal center is selective toward the ligand L^B/L^{B*} including a hexahydropyrimidine (imidazolidine) ring and the shorter ethylene (longer propylene) bridge. The Fe^{II} cation is small enough to exert a template effect, resulting in the ring opening of L^B/L^{B*}. The resulting bis-Schiff base $L^{B'}$ is stabilized through pentacoordination, yielding $[Fe^{II}L^{B'}(NCS)](NCS)$ (**2**). Ni^{II} is too bulky to promote the ring opening of L^B/L^{B*}: L^B acts as a tetradentate ligand, yielding $[Ni^{II}L^B(NCS)_2]$ (**5**) (the L^{B*} isomer is totally converted to L^B). The coordinative requirements and stereochemical preference of the bulkier Zn^{II} cation allow neither the ring opening of L^B/L^{B*} nor the tetracoordination of L^B or L^{B*} but stabilize the novel tetradentate dissymmetric form $L^{B°}$ in $[Zn^{II}L^{B°}(NCS)_2]\cdot H_2O$ (**8**) ($L^{B°}$ results from MeOH addition across the imine bond of L^B). Density functional theory calculations performed for Ni^{II} and Zn^{II} complexes of the $L^B/L^{B*}/L^{B°}$ set of ligands allowed one to compare the relative stabilities of all possible isomers, showing that the most stable ones correspond to those experimentally obtained: isomerization, or methanol addition across the imine bond, of the tetradentate ligand depends on the relative stabilities of all possible isomeric complexes.

Introduction

Pioneering work on the preparation of imidazolidines through the 1:1 condensation reaction of aldehydes and 1,2-diamines was carried out as early as the end of the 19th to the beginning of the 20th century[1−4] and comprehensively reviewed in 1954.[5] Later, a reaction mechanism has been proposed accounting for the fact that, while 1,2-diamines in which both amino groups are secondary yield exclusively imidazolidines, 1,2-diamines containing one secondary and one primary amino group may yield either exclusively imidazolidines or mixtures of imidazolidine and the isomeric acyclic Schiff base, with relative ratios depending on the aldehyde and diamine substituents.[6] Their uses, including therapeutic properties, have been reported.[5,7]

* To whom correspondence should be addressed. E-mail: tuchague@lcc-toulouse.fr. Fax: (+33)561553003.

† On leave from the Institute of Applied Physics, Academy of Sciences of Moldova, Academiei strasse 3, 2028 Chisinau, Moldova.

(1) (a) Moos, F. *Ber. Dtsch. Chem. Ges.* **1887**, *20*, 732−735. (b) van Alphen, J. *Recl. Trav. Chim. Pays-Bas* **1935**, *54*, 93−96; **1936**, *55*, 669−674. (c) Lob, G. *Recl. Trav. Chim. Pays-Bas* **1936**, *55*, 859−873. (d) Rameau, J. Th. L. B. *Recl. Trav. Chim. Pays-Bas* **1938**, *57*, 192−214. (e) Donia, R. A.; Shotton, J. A.; Bentz, L. O.; Smith, G. E. P., Jr. *J. Org. Chem.* **1949**, *14*, 952−961. (f) Billman, J. H.; Chen Ho, J. Y.; Caswell, L. R. *J. Org. Chem.* **1952**, *17*, 1375−1378. (g) Wanzlick, H. W.; Lochel, W. *Chem. Ber.* **1953**, *86*, 1463−1466. (h) Jaunin, R. *Helv. Chim. Acta* **1960**, *43*, 561−566. (i) Kahwa, I. A.; Fronczek, F. R.; Selbin, J. *Inorg. Chim. Acta* **1988**, *148*, 273−281.

(2) (a) van Alphen, J. *Recl. Trav. Chim. Pays-Bas* **1936**, *55*, 412−418. (b) Liu, S.; Wong, E.; Rettig, S. J.; Orvig, C. *Inorg. Chem.* **1993**, *32*, 4268−4276. (c) Wong, E.; Liu, S.; Lügger, T.; Hahn, F. E.; Orvig, C. *Inorg. Chem.* **1995**, *34*, 93−101. (d) Yiang, L.-W.; Liu, S.; Wong, E.; Rettig, S. J.; Orvig, C. *Inorg. Chem.* **1995**, *34*, 2164−2178.

10.1021/ic050791b CCC: $30.25
Published on Web 10/25/2005

Except for this conventional preparation method, imidazolidine rings may be generated by ring contraction of large coordinated macrocyclic Schiff bases upon substitution of bulky alkaline-earth cations by smaller transition-metal ions.[8] All imidazolidine rings reported above as generated upon ring contraction required coordination of the large macrocyclic Schiff bases from which they were formed. A notable exception to this is the report of Menif et al.[9] showing that direct 2:2 condensation of isophthaldehyde and diethylenetriamine produces a mixture of two isomers: a macrocycle made from an 18-membered inner ring (including two imine bonds) and two 5-membered imidazolidine outer rings and a hexaaza 24-membered macrocycle including four imine and two secondary amine bonds. Reaction of this ligand mixture with copper ions fully shifts this equilibrium toward the coordinated hexaaza 24-membered macrocycle (Schiff base isomer).

Diethylenetriamine has also been reacted in a 1:2 mole ratio with *p*-nitrobenzaldehyde to yield the first acyclic ligand including both a Schiff base imine linkage and an imidazolidine ring.[10] More recently, the same type of double condensation reaction has been carried out between 2-pyridinecarboxaldehyde *N*-oxide and diethylenetriamine, triethylenetetramine, and 3,3′-iminobis(propylamine), quantitatively yielding, in all three cases, condensation products including saturated heterocycle(s) rather than the isomeric bis-Schiff bases. The authors interpreted this result as arising from preliminary formation of the corresponding bis-Schiff bases followed by their isomerization to the obtained compounds.[11] In subsequent papers, Boča et al.[12] showed that complexation of the ligands containing imidazolidine ring(s) with transition-metal ions is accompanied by ring(s) opening.

Our interest in novel dissymmetric polydentate nitrogen ligands led us to explore the reaction between 2-pyridinecarboxaldehyde and diethylenetriamine, 3-[(2-aminoethyl)amino]propylamine, and 3,3′-iminobis(propylamine) in a 2:1 molar ratio. Indeed, such ligands including several functions (amine, imine, pyridine, imidazoline, and hexahydropyrimidine) able to provide nitrogen donors allowing tuning of the ligand field are of great interest for spin-crossover compounds. The only imidazolidine derivative previously prepared from 2-pyridinecarboxaldehyde was reported by Castle and involved a 1,2-diamine.[13] On the other hand, the 2:1:1 reaction of 2-pyridinecarboxaldehyde, an α,ω-triamine, and a metal salt has been reported to yield complexes of the corresponding acyclic bis-Schiff bases: Zn[14] and Ru[15] complexes for diethylenetriamine, Mn[16] and Cu[17] complexes for 3-[(2-aminoethyl)amino]propylamine, and Mn,[16,18] Co,[19] and Ni[20] complexes for 3,3′-iminobis(propylamine). However, no solution or solid-state structural information that could help in distinguishing between the acyclic bis-Schiff base and cyclic imidazolidine (hexahydropyrimidine) isomeric forms of these ligands is available.

Chart 1. Possible Products from the 2:1 Condensation Reaction of 2-Pyridinecarboxaldehyde with Diethylenetriamine

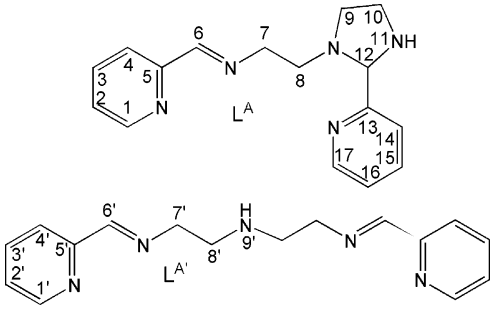

Depending on the length of the carbon chains between the central secondary and the two terminal primary amine functions and on the stability of the five-membered (imidazolidine) or six-membered (hexahydropyrimidine) rings, the reaction products sketched in Charts 1−3 are expected from the reaction (2:1 molar ratio) between 2-pyridinecarboxaldehyde and diethylenetriamine, 3-[(2-aminoethyl)amino]-propylamine, and 3,3′-imino(bispropylamine), respectively.

In this paper, we describe the synthesis and characterization of the novel dissymmetric polydentate ligands: *N*-[2-(2-pyridin-2-ylimidazolidin-1-yl)ethyl]-*N*-(1-pyridin-2-ylmethylene)amine (L^A), *N*-(1-pyridin-2-ylmethylene)-*N*-[2-(2-pyridin-2-yltetrahydropyrimidin-1(2*H*)-yl)ethyl]amine (L^B), *N*-[3-(2-pyridin-2-ylimidazolidin-1-yl)propyl]-*N*-(1-pyridin-2-ylmethylene)amine (L^{B*}), and *N*-(1-pyridin-2-ylmethylene)-

(3) (a) Riebsomer, J. L. *J. Org. Chem*. **1950**, *15*, 237−240. (b) Ferm, R. J.; Riebsomer, J. L.; Martin, E. L.; Daub, G. H. *J. Org. Chem*. **1953**, *18*, 643−648.
(4) (a) Mason, A. T. *Ber. Dtsch. Chem. Ges*. **1887**, *20*, 267−277. (b) Strache, H. *Ber. Dtsch. Chem. Ges*. **1888**, *21*, 2358−2369. (c) Kolda, E. *Monatsh. Chem*. **1898**, *19*, 609−626.
(5) Ferm, R. J.; Riebsomer, J. L. *Chem. Rev*. **1954**, *54*, 593−613.
(6) Chapuis, C.; Gauvreau, A.; Klaebe, A.; Lattes, A.; Périé, J. J. *Bull. Soc. Chim. Fr*. **1973**, 977−985.
(7) Billman, J. H.; Khan, M. S. *J. Pharm. Sci*. **1968**, *7*, 1817−1819.
(8) (a) Nelson, S. M.; Esho, F. S.; Drew, M. G. B.; Bird, P. *J. Chem. Soc., Chem. Commun*. **1979**, 1035−1037. (b) Nelson, S. M.; Knox, C. V.; McCann, M.; Drew, M. G. B. *J. Chem. Soc., Dalton Trans*. **1981**, 1669−1677. (c) Drew, M. G. B.; Nelson, J.; Nelson, S. M. *J. Chem. Soc., Dalton Trans*. **1981**, 1678−1684. (d) Drew, M. G. B.; Nelson, J.; Nelson, S. M. *J. Chem. Soc., Dalton Trans*. **1981**, 1691−1696. (e) Nelson, S. M.; Esho, F. S.; Drew, M. G. B. *J. Chem. Soc., Dalton Trans*. **1982**, 407−415. (f) Bailey, N. A.; Eddy, M. M.; Fenton, D. E.; Moss, S.; Mukhopadhyay, A.; Jones, G. *J. Chem. Soc., Dalton Trans*. **1984**, 2281−2288. (g) Guerriero, P.; Casellato, U.; Tamburini, S.; Vigato, P. A.; Graziani, R. *Inorg. Chim. Acta* **1987**, *129*, 127−138. (h) Fenton, D. E.; Vigato, P. A. *Inorg. Chim. Acta* **1987**, *139*, 39−48. (i) Adams, H.; Bailey, N. A.; Bertrand, P.; Collinson, S. R.; Fenton, D. E.; Kitchen, S. J. *J. Chem. Soc., Dalton Trans*. **1996**, 1181−1183.
(9) Menif, R.; Martell, A. E.; Squattrito, P. J.; Clearfield, A. *Inorg. Chem*. **1990**, *29*, 4723−4729.
(10) Tamburini, S.; Vigato, P. A.; Casellato, U.; Graziani, R. *J. Chem. Soc., Dalton Trans*. **1989**, 1993−2002.
(11) Boča, M.; Valigura, D.; Linert, W. *Tetrahedron* **2000**, *56*, 441−446.
(12) (a) Boča, M.; Baran, P.; Boča, R.; Fuess, H.; Kickelbick, G.; Linert, W.; Renz, F.; Svoboda, I. *Inorg. Chem,* **2000**, *39*, 3205−3212. (b) Boča, M.; Valko, M.; Kickelbick, G.; Ďurik, M.; Linert, W. *Inorg. Chim. Acta* **2003**, *349*, 111−122.
(13) Castle, R. N. *J. Org. Chem*. **1958**, *23*, 69−71.
(14) Itoh, Y. *Bunseki Kagaku* **1983**, *32*, E25−E32.
(15) Cheng, C. C.; Lu, Y. C.; Lo, C. C. *Bull. Inst. Chem., Acad. Sin*. **1997**, *44*, 61−69.
(16) Coleman, W. M.; Taylor, L. T. *J. Inorg. Nucl. Chem*. **1979**, *41*, 95−98.
(17) Sakurai, T.; Kimura, M.; Nakahara, A. *Bull. Chem. Soc. Jpn*. **1981**, *54*, 2976−2978.
(18) Lau, S. H.; Caps, V.; Young, K. W.; Tsang, S. C. *Microporous Mesoporous Mater*. **1999**, *32*, 279−285.
(19) (a) Spencer, C. T.; Taylor, L. T. *Inorg. Chem*. **1973**, *12*, 644−648. (b) Laurence, G. A. *Polyhedron* **1985**, *4*, 599−601. (c) Hay, R. W.; Novan, N. *J. Indian Chem. Soc.* **1992**, *69*, 495−500.
(20) Coleman, W. M., III. *Inorg. Chim. Acta* **1981**, *49*, 205−208.

Chart 2. Possible Products from the 2:1 Condensation Reaction of 2-Pyridinecarboxaldehyde with 3-[(2-Aminoethyl)amino]propylamine

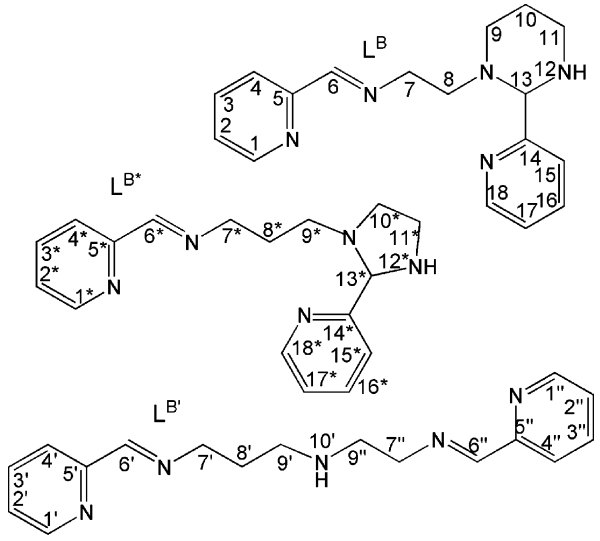

Chart 3. Possible Products from the 2:1 Condensation Reaction of 2-Pyridinecarboxaldehyde with 3,3′-Iminobis(propylamine)

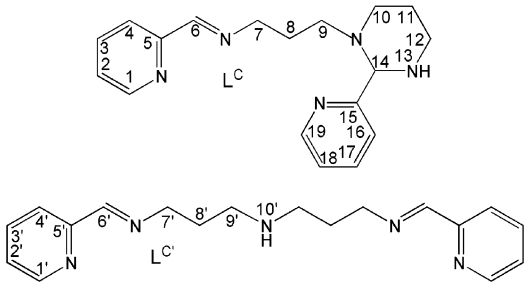

Chart 4. Tetradentate Ligand L^{B°

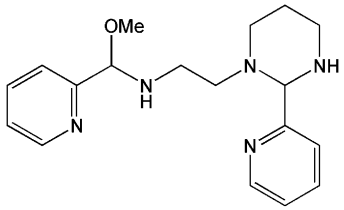

N-[3-(2-pyridin-2-yltetrahydropyrimidin-1(2*H*)-yl)propyl]-amine (L^C). The synthesis and characterization of three Fe^{II} complexes, $Fe^{II}L(NCS)_2$ ($L = L^A$, $L^{B'}$, or $L^{C'}$), three Ni^{II} complexes, $Ni^{II}L(NCS)_2$ ($L = L^A$, L^B, or $L^{C'}$), and three Zn^{II} complexes, $Zn^{II}L(NCS)_2$ ($L = L^A$, L^{B°, or L^C) have also been carried out including single-crystal X-ray molecular structure determination for six of them and IR, conductivity, magnetic, and Mössbauer studies. The tetradentate ligand *N*-[methoxy-(pyridin-2-yl)methyl]-*N*′-(2-pyridin-2-yltetrahydropyrimidin-1(2*H*)-yl)ethane-1,2-diamine (L^{B°), identified in $Zn^{II}L^{B^\circ}(NCS)_2$ but not isolated, is sketched in Chart 4.

The respective roles of the polydentate ligand L and of the metal ion (Fe^{II}, Ni^{II}, and Zn^{II}) in yielding this variety of metal complexes through isomerization reactions of L, plus (in one case) methanol addition, are analyzed on the basis of the obtained structural and spectroscopic data. Density functional theory (DFT) calculations are performed to evaluate the possible origin for the specific isomer selectivities.

Isolated Ligands: Results and Discussion

The condensation products resulting from the reaction between 2-pyridinecarboxaldehyde and diethylenetriamine, 3-[(2-aminoethyl)amino]propylamine, and 3,3′-iminobis(propylamine) in a 2:1 molar ratio were isolated as light-brown oils. Their NMR spectra (^1H and ^{13}C) were fully assigned (Experimental Section) on the basis of comparisons with ^1H NMR spectra of the symmetrical bis(2-pyridyl)iminoethylene ligand[21] and of selective irradiations in the 7−9 ppm range.

The ^{13}C NMR spectra of the reaction products corresponding to Charts 1 and 3 include 16 and 18 distinct signals, respectively, thus excluding the symmetrical isomers $L^{A'}$ and $L^{C'}$ and suggesting the presence of only dissymmetric cyclic isomers L^A and L^C. The conclusive criterion allowing one to prove the presence of the five-membered (imidazolidine) or six-membered (hexahydropyrimidine) saturated rings of L^A and L^C, respectively, is given by the carbon atom directly bonded to the pyridine ring [δ(C12) = 83.4 ppm in L^A and δ(C14) = 82.0 ppm in L^C]. In the case of saturated rings, this carbon is sp^3-hybridized and a ^{13}C NMR chemical shift range of 70−90 ppm is expected as a result of its position between two nitrogen atoms. In the isomeric Schiff base, the corresponding carbon atom is sp^2 and a ^{13}C NMR chemical shift range of 150−160 ppm is then expected; moreover, the $^1HC{=}N$ resonance of the isomeric Schiff base is then expected at ∼8.3 ppm. The values δ(H12) = 4.21 ppm in L^A and δ(H14) = 4.00 ppm in L^C definitely confirm the presence of the saturated imidazolidine (L^A) and hexahydropyrimidine (L^C) rings. Complete assignment of their ^{13}C and ^1H NMR spectra (Experimental Section) proved the quantitative formation of the dissymmetric isomers including the imidazolidine (L^A) and hexahydropyrimidine (L^C) rings.

The ^1H and ^{13}C NMR spectra of the reaction product corresponding to Chart 2 include both sets of absorptions previously assigned to L^A and L^C. This observation is in line with the likely equilibrium between the dissymmetric isomers L^B and L^{B*} (including the hexahydropyrimidine and imidazolidine ring, respectively). A ∼60% ratio of L^{B*} was evaluated through integration of selected ^1H NMR signals.

To summarize, the condensation products resulting from the reaction between 2-pyridinecarboxaldehyde and diethylenetriamine, 3-[(2-aminoethyl)amino]propylamine, and 3,3′-iminobis(propylamine) in a 2:1 molar ratio are not bis-Schiff bases but their dissymmetric isomers containing one saturated heterocyclic ring, L^A, L^B/L^{B*}, and L^C.

This result seems to be quite general and in line with the one described by Boča et al.,[11] who showed that reactions between 2-pyridinecarboxaldehyde-*N*-oxide and diethylenetriamine, triethylenetetramine, or 3,3′-iminobis(propylamine) quantitatively yield, in all three cases, condensation products including saturated heterocycle(s) rather than the isomeric bis-Schiff bases. These authors considered that stabilization of the obtained cyclic condensation products originates from intramolecular hydrogen bonds between the imidazolidine NH groups and the oxygen atoms of the pyridine *N*-oxide

(21) Costes, J.-P.; et al., unpublished results.

Scheme 1. Possible Mechanisms Yielding the Imidazolidine Derivative Resulting from 1:1 Condensation of Pyridinecarboxaldehyde and Diethylenetriamine

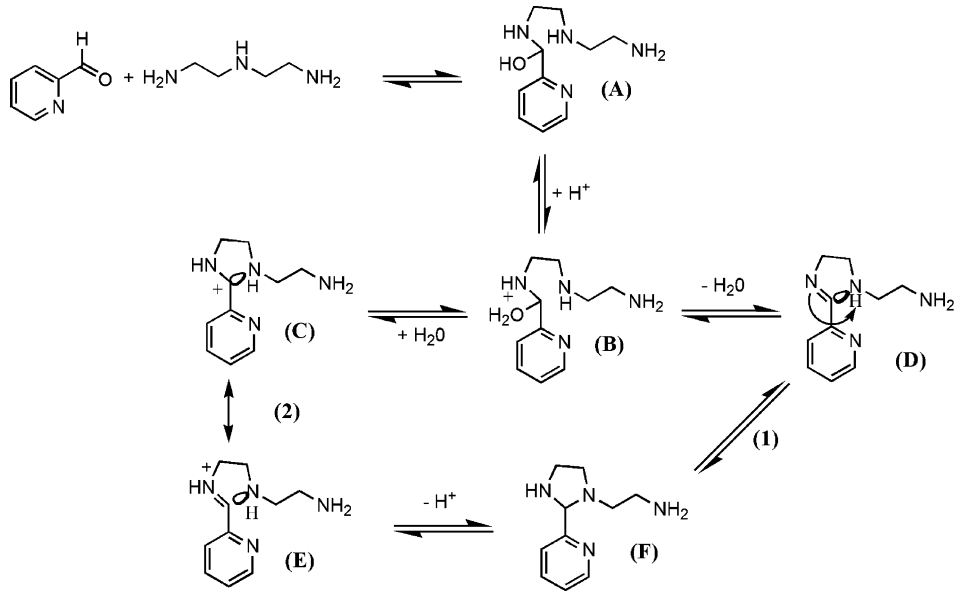

and suggested that formation of the cyclic condensation products involves the following sequence of reactions: (i) Schiff base condensation and (ii) nucleophilic addition of the nitrogen atom (secondary amine group) to the electrophilic $C^{\delta+}$ (imine) accompanied by proton transfer. However, in the case of L^A, L^B/L^{B*}, and L^C, which include a terminal pyridine instead of the terminal pyridine *N*-oxide, no intramolecular hydrogen bond can be established, ruling out the possibility for such stabilization of the cyclic isomers. Moreover, if we consider previously reported results,[9,10,13] again the lack of intramolecular hydrogen bonds in the reported species rules out the argument of Boča et al.[11] that cyclic isomers are the final products because they are stabilized through an intramolecular hydrogen bond. On the other hand, our observations, together with previous ones,[9,10,13] suggest that the stability of the cyclic isomer is an intrinsic and general feature in the condensation reaction involving aldehydes and polyamines containing at least one secondary group and one primary amino group. Then, considering the weak stability of Schiff bases, it is possible to envision a mechanism involving the following sequence of reactions: (i) 1:1 condensation of the α,ω-triamine with 2-pyridinecarboxaldehyde, (ii) nucleophilic addition yielding the cyclic isomer as sketched in Scheme 1 for the specific example of L^A, and (iii) Schiff base condensation involving the terminal NH_2 group of fragment **F**.

The mechanism sketched in Scheme 1 is based on the formation of the hemiaminal (**A**) resulting from nucleophilic attack of nitrogen and prototropy, as a first step; consecutive addition of proton yields form **B**. Then two routes are possible: addition of water leads to the carbocation (**C**) stabilized by conjugation, whereas, alternately, direct elimination of water yields form **D**. The iminium form (**E**) yields the imidazolidine intermediate (**F**) upon cyclization and deprotonation.

This sequence of reactions is more plausible than the mechanism proposed by Boča et al., which considers that a bis-Schiff base is formed prior to cyclization to imidazolidine. Indeed, our suggested mechanism involves a cyclic intermediate (**F**) in a consecutive bimolecular reaction, which is more likely to occur than that leading directly to the less stable isomeric Schiff base. Obtaining almost equimolar amounts of isomers L^B and L^{B*} (Chart 2) may be explained by the equilibrium between (or statistical formation of) the two hemiaminals.

Complexes: Results

The novel dissymmetric polydentate nitrogen ligands L^A, L^B/L^{B*}, and L^C were treated with three different metal ions, Fe^{II}, Ni^{II}, and Zn^{II}, in order to explore their coordinating ability and the stability of their different isomeric forms upon complexation, as a result of both the compared ligand characteristics (for a given metal ion) and the metal ion effect (for a given ligand). All complexation reactions were carried out in the same solvent (methanol) in the presence of the same coordinating anion, thiocyanate. Nine complexes having the same overall composition $ML(NCS)_2$ ($M = Fe^{II}$, Ni^{II}, or Zn^{II}; $L = L^A$, L^B, or L^C) were reproducibly obtained. On the basis of their extensive study (next subsections), they were unambiguously characterized as $Fe^{II}L(NCS)_2$ [$L = L^A$ (**1**), $L^{B'}$ (**2**), or $L^{C'}$ (**3**)], $Ni^{II}L(NCS)_2$ [$L = L^A$ (**4**), L^B (**5**), or $L^{C'}$ (**6**)], and $Zn^{II}L(NCS)_2$ [$L = L^A$ (**7**), L^{B° (**8**), or $L^{C'}$ (**9**)].

Description of the Structures. The crystal structures of $[Fe^{II}L^A(NCS)_2]$ (**1**), $[Fe^{II}L^{C'}(NCS)](NCS)$ (**3**), $[Ni^{II}L^A(NCS)_2]$ (**4**), $[Ni^{II}L^B(NCS)_2]$ (**5**), $[Ni^{II}L^{C'}(NCS)](NCS)$ (**6**), and $[Zn^{II}L^{B^\circ}(NCS)_2]\cdot H_2O$ (**8**) have been determined by single-crystal X-ray diffraction analyses.

Crystal Structures of 1 and 4. Complexes **1** and **4** have similar compositions and are isostructural with a neutral $[M^{II}L^A(NCS)_2]$ asymmetric unit. As an example, the structure of **1**, illustrated in Figure 1, is described.

The N_6 donor set to the metal center is a slightly distorted octahedron including one imine, one imidazolidine, and two

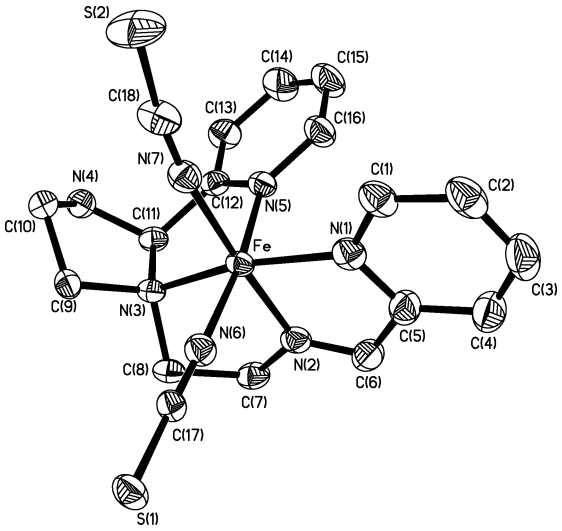

Figure 1. Molecular structure of **1** with an atom labeling scheme. Thermal ellipsoids are drawn at the 50% probability level. Selected bonds distances (Å) (*for the corresponding isomorphous $[Ni^{II}L^{A}(NCS)_2]$ complex **4**): M−N1, 1.974(2) [*2.114(4)]; M−N2, 1.882(2) [*2.026(4)]; M−N3, 2.040(2) [*2.150(4)]; M−N5, 1.963(2) [*2.078(4)]; M−N6, 1.958(2) [*2.082(4)]; M−N7, 1.955(2) [*2.027(4)].

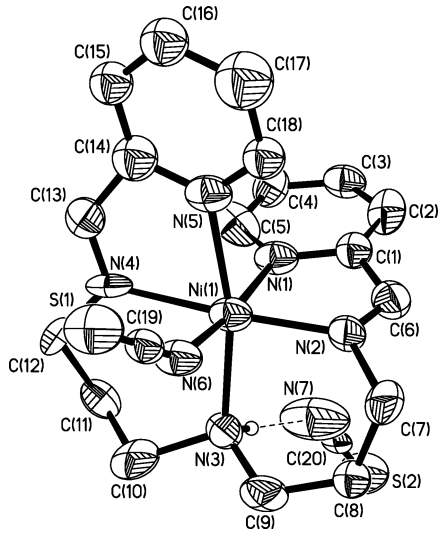

Figure 2. Molecular structure of **6** with an atom labeling scheme. Thermal ellipsoids are drawn at the 50% probability level. Selected bonds distances (Å) (*for the corresponding isomorphous $[Fe^{II}L^{C'}(NCS)](NCS)$ complex **3**): M−N1, 2.120(8) [*1.970(7)]; M−N2, 1.922(11) [*1.937(10)]; M−N3, 2.126(10) [*2.057(11)]; M−N4, 2.130(13) [*1.939(10)]; M−N5, 2.118(8) [*1.926(8)]; M−N6, = 2.067(8) [*1.951(6)].

pyridine nitrogen donors from the folded dissymmetric tetradentate L^A ligand and one nitrogen donor from each thiocyanate anion; the thiocyanate anions are thus cis-coordinated. The Fe−N bonds lengths (Figure 1) are typical of low-spin (LS) Fe^{II}. The Fe−N−C meta−thiocyanate bond angles [174.2(4)° and 177.8(4)° for N6 and N7, respectively] are close to 180°. The Fe1−N1−C5−C6−N2 and Fe1−N3−C11−C12−N5 metallacycles are conjugated and have a nearly planar conformation. The Fe1−N2−C7−C8−N3 metallacycle has an envelope conformation: C8 deviates by 0.30 Å from the mean Fe1,N2,C7,N3 plane toward N6(NCS). The five-membered N3−C9−C10−N4−C11 imidazolidine ring also has an envelope configuration, where C10 deviates by 0.57 Å toward N7(NCS). Despite significant differences in the M−N bond lengths between complexes **1** (average Fe−N = 1.962 Å) and **4** (average Ni−N = 2.080 Å), the dissymmetric isomeric form L^A of the ligand including one imidazolidine ring and one (short) ethylene bridge is stabilized through tetracoordination in both complexes. The crystal packing essentially results from several C−H···S intermolecular contacts[22] (3.52−3.76 Å range) between adjacent $[ML^A(NCS)_2]$ molecules.

Crystal Structures of 3 and 6. Complexes **3** and **6** have the same composition and are isostructural with an asymmetric unit including a $[M^{II}L^{C'}(NCS)]^+$ cation and a thiocyanate counteranion. As an example, the structure of **6**, illustrated in Figure 2, is described.

The N_6 donor set to the metal center is a slightly distorted octahedron including one amine, two imine, and two pyridine nitrogen donors from the symmetric pentadentate $L^{C'}$ ligand and one thiocyanate nitrogen donor. The Fe−N bond lengths (Figure 2) are typical of LS Fe^{II}. Despite significant differences in the M−N bond lengths between complexes **3** (average Fe−N = 1.963 Å) and **6** (average Ni−N = 2.081 Å), the symmetric isomeric form $L^{C'}$ of the ligand including the larger propylene bridges is stabilized through penta-coordination in both complexes. The $[M^{II}L^{C'}(NCS)]^+$ cationic species and thiocyanate counteranion are hydrogen-bonded (N3−H = 0.90 Å, H···N7 = 2.14(3) Å, and N3−H−N7 = 177.2°). The crystal packing essentially results from these hydrogen contacts and S1···S2′ (x, y, $z - 1$) interactions[23] between coordinated and noncoordinated (but hydrogen-bonded) NCS anions of adjacent asymmetric units along c (3.43 and 3.49 Å for **3** and **6**, respectively).

Crystal Structures of 5 and 8. Although they have been prepared from the same ligand mixture (L^B/L^{B*}; see the Isolated Ligands section), complexes **5** and **8** have different compositions and are not isostructural. However, their asymmetric units, shown in Figure 3a for **5** and in Figure 3b for **8**, are similar in the sense that they are neutral $[M^{II}L(NCS)_2]$ species, where L is a dissymmetric tetradentate ligand and the two thiocyanate anions are cis-coordinated.

The essential difference between **5** and **8** originates from the nature of the L ligand: L^B is the novel dissymmetric ligand including a hexahydropyrimidine ring, depicted in Chart 2, and $L^{B°}$, depicted in Chart 4, derives from L^B through the addition of methanol across the azomethine bond, thus converting the imine double bond of L^B into a more flexible single C−N bond. Indeed, while the C6−N2 bond length is 1.246(7) Å in **5**, it is equal to 1.444(8) Å in **8**, in agreement with the imine and amine character of N2 in complexes **5** and **8**, respectively. For both complexes, the metal center is in a slightly distorted N6 coordination environment involving one hexahydropyrimidine, one imine (**5**) [or one amine (**8**)], two pyridine nitrogen donors from the folded dissymmetric tetradentate ligand L^B (**5**) [or $L^{B°}$

(22) (a) Desiraju, G. R.; Nalini, V. *J. Mater. Chem.* **1991**, *1*, 201−203. (b) van Derberg, J.-A.; Seddon, K. R. *Cryst. Growth Des.* **2003**, *3*, 643−661. (c) Desiraju, G. R. *Chem. Commun.* **2005**, 2995−3001.

(23) Takahashi, K.; Kawakami, T.; Gu, Z.-Z.; Einaga, Y.; Fujishima, A.; Sato, O. *Chem. Commun.* **2003**, 2374−2375.

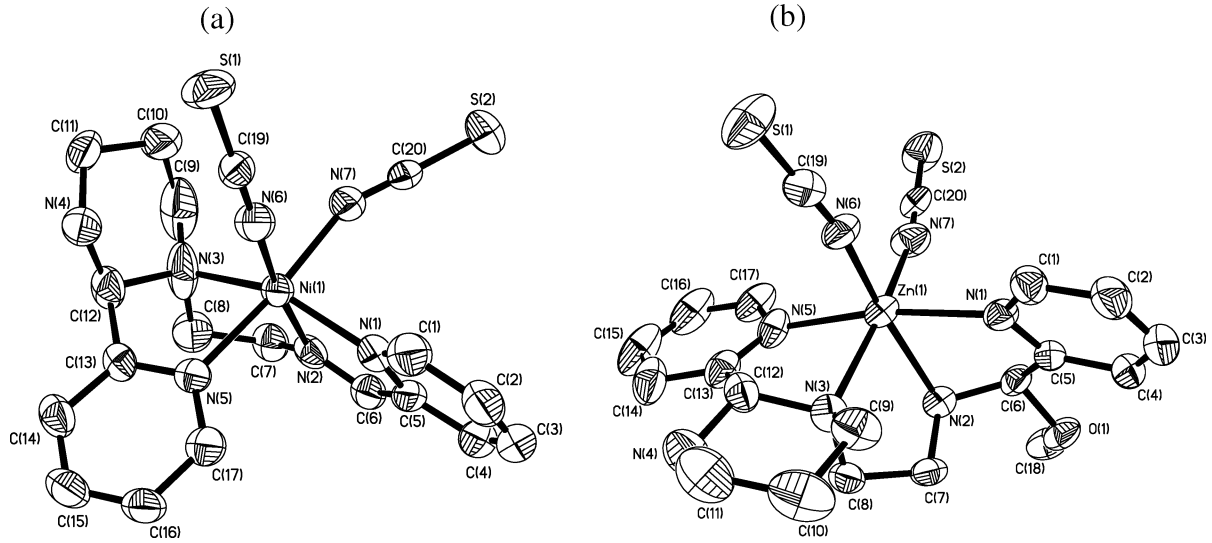

Figure 3. Molecular structures of (a) **5** and (b) **8** with atom labeling schemes. Thermal ellipsoids are drawn at the 50% probability level. Selected bonds distances (Å): (a) Ni−N1, 2.085(4); Ni−N2, 2.036(3); Ni−N3, 2.172(4); Ni−N5, 2.114(3); Ni−N6, 2.045(4); Ni−N7, 2.070(4); (b) Zn−N1, 2.185(5); Zn−N2, 2.221(5); Zn−N3, 2.238(5); Zn−N5, 2.173(5); Zn−N6, 2.075(5); Zn−N7, 2.085(6).

(**8**)], and one nitrogen donor from each thiocyanate anion; the thiocyanate anions are thus cis-coordinated.

The structure of complexes **5** and **8** also differ in the relative positions of the pyridine rings, which are cis to each other in **5** and trans to each other in **8**. This difference may originate from the different conformations of the five-membered M−N1−C5−C6−N2 metallacycles: in **5**, Ni−N1−C5−C6−N2 is conjugated and planar (atom distances within the estimated standard deviations from the least-squares plane); in **8**, where Zn−N1−C5−C6−N2 is saturated and nonplanar, the flexibility of L^{B° is obviously increased as compared to L^B in **5**. The six-membered hexahydropyrimidine rings have the same chair conformation in complexes **5** and **8**. The solvate water molecule in **8** is disordered over two equivalent positions and is not involved in H bonds. The values of the shorter intermolecular contacts indicate that the neutral molecules of complexes **5** and **8** are not involved in H bonds, S···S contacts, or π-stacking interactions and their packing in the crystal may result from van der Waals interactions.

The dissymmetric forms L^B and L^{B° of the ligand including one hexahydropyrimidine ring and one short ethylene bridge are stabilized through tetracoordination. Nucleophilic attack of a C═N imine by methanol has been reported in large coordinated macrocyclic Schiff bases and interpreted as resulting from a mismatch of the cavity size of the macrocycle with the size of the coordinated metal cation.[8a,b] It may then be suggested that while six-coordinate Ni^{II} (ionic radius $r = 83$ pm)[24] matches the bite angles of L^B, six-coordinate Zn^{II} ($r = 88$ pm)[24] is too bulky for allowing tetracoordination of L^B, thus favoring the nucleophilic attack of the C═N imine by methanol.

NMR Solution Studies. The NMR spectra (^{1}H and ^{13}C) of the iron and nickel complexes showed very broad resonances, which could not yield any information on the isomeric form(s) of the ligand present in solution. Although the NMR spectra (^{1}H and ^{13}C) of the zinc complexes could not be fully assigned, some useful information could be obtained with regard to the isomeric form(s) of the ligand present in solution. While the NMR spectra of complexes **7** and **8** (L = L^A and L^{B°, respectively) were similar and included a large number of superimposed resonances (not taking into account the possible isomeric forms described in the DFT Calculations section, the dissymmetric ligands L^A and L^{B° should have twice as many resonances as their symmetrical isomers), those of complex **9** were simpler, allowing their overall assignment to the acyclic symmetric bis-Schiff base isomeric form $L^{C'}$ of the ligand. This overall assignment was supported by the absence of a resonance attributable to the H14 hexahydropyrimidine proton for complex **9**, while resonances attributable to the H12 imidazolidine (**7**) or H15 hexahydropyrimidine (**8**) protons were observed.

Table 1. Infrared Attributions of Significant Vibrations for Complexes **1**−**9**[a]

complex	ν(NH)	ν(N═C)	ν(N═C)$_{pyr}$	ν(NCS)
1	3253 (m)	1646 (w)	1600 (m)	2110 (s)
2	3120 (m)	1634 (s)	1602 (m)	2052−2085 (s)
3	3128 (m)	1650 (s)	1603 (m)	2049−2089 (s)
4	3264 (m)	1663 (m)	1600 (m)	2087 (s)
5	3312 (m)	1670 (m)	1602 (s)	2089 (s)
6	3160 (m)	1642 (s)	1599 (m)	2050−2077 (s)
7	3250 (m)	1653 (w)	1601 (s)	2068 (s)
8	3237 (m)		1601 (s)	2083 (s)
9	3161 (m)	1654 (s)	1595 (m)	2050−2071 (s)

[a] s: strong. m: medium. w: weak.

IR Spectroscopy and Conductivity. Infrared wavenumbers (cm^{-1}) of significant valence vibrations helpful for identification of the ligands and of coordinated or out-of-sphere NCS anions are collated in Table 1.

In agreement with the literature data,[11,12] N−H valence vibrations of cyclic secondary amines (imidazolidine and hexahydropyrimidine) are observed in the 3237−3312 cm^{-1} range for structurally characterized complexes **1**, **4**, **5**, and **8**

(24) Huheey, J. E. *Inorganic Chemistry*, 2nd ed.; Harper & Row: New York, 1978; pp 71−74.

containing ligands L^A, L^B, or L^{B°. In addition, the presence of a broad absorption in the 2000−2100 cm^{-1} range, characteristic of two cis-coordinated thiocyanate anions,[25] is in agreement with the structures of **1**, **4**, **5**, and **8**. From the values ν(NH) = 3250 cm^{-1} and ν(NCS) = 2068 cm^{-1}, it may thus be deduced that complex **7** includes the tetradentate L^A ligand (dissymmetric imidazolidine-containing isomer; Chart 1) and two cis-coordinated NCS anions. The molar conductivity (Experimental Section) for complex **7** (138 S cm^2 mol^{-1}) is close to that of **8** (128 S cm^2 mol^{-1}) but higher than those of **1**, **4**, and **5** (66−75 S cm^2 mol^{-1}). While the structure of **8** and IR spectra of **7** and **8** show unambiguously that both SCN− ligands are coordinated in the solid state, it is likely that in solution one of the SCN− ligands is replaced by a molecule of solvent.

N−H valence vibrations of aliphatic secondary amine functions (symmetric Schiff base isomer $L^{C'}$; Chart 3) in structurally characterized complexes **3** and **6** are found at frequencies (3128 and 3160 cm^{-1}, respectively) lower than usually observed.[11,12,26] The strong N−H···N hydrogen bonds between secondary amine functions and noncoordinated NCS groups shift the ν(N−H) of $L^{C'}$ to lower frequency. The presence of two resolved absorptions in the 2000−2100-cm^{-1} range clearly indicates the presence of two distinct thiocyanate groups, in agreement with the structure of complexes **3** and **6**, which show one coordinated anion and one out-of-sphere NCS anion. From the values ν(NH) = 3120 (**2**) and 3161 (**9**) cm^{-1} and ν(NCS) = 2052 and 2085 cm^{-1} (**2**) and 2050 and 2071 cm^{-1} (**9**), it may thus be deduced that (a) complex **2** includes the pentadentate $L^{B'}$ ligand (Schiff base isomer; Chart 2), (b) complex **9** includes the pentadentate $L^{C'}$ ligand (symmetric Schiff base isomer; Chart 3), and (c) **2** and **9** include one coordinated anion and one out-of-sphere NCS anion. The molar conductivity of complexes **2** and **9** (138 and 190 S cm^2 mol^{-1}, respectively)[27] further confirms their monocationic character as proposed on the basis of the IR data.

In agreement with previously reported data,[11,12b,26] C═N(Schiff base) absorptions are in the 1670−1634-cm^{-1} range, and C═N(pyridine) absorptions are in the 1603−1595-cm^{-1} range. In keeping with the structural data showing the presence of ligand L^{B° (Chart 4) in complex **8**, there is no C═N(Schiff base) absorption in the IR spectrum of complex **8**.

Magnetic Properties. The 295 K magnetic moments of complexes **1**−**3** are ∼0 μ_B, confirming the LS state of Fe^{II} evidenced by the molecular structures of **1** and **3**. The 295 K magnetic moments of complexes **4**−**6** are in the 2.9−3.2 μ_B range, close to the 2.83 μ_B spin-only value characteristic of the O_h Ni^{II} symmetry evidenced by the molecular structures of **4**−**6**.

Mössbauer Spectroscopy. In agreement with the magnetic data, the room-temperature Mössbauer spectra of complexes **1**−**3** evidence a unique quadrupole-split doublet with parameters (isomer shifts, δ, and quadrupole splittings, ΔE_Q) characteristic of LS Fe^{II}.[28] The Mössbauer parameters of the neutral $[FeL^A(NCS)_2]$ complex **1** with two cis-coordinated thiocyanate anions in the coordination sphere [δ = 0.313(2) and ΔE_Q = 0.730(4) mm s^{-1}] are not significantly different from those of the cationic $[FeL^{C'}(NCS)](NCS)$ complex **3** [δ = 0.268(3) and ΔE_Q = 0.838(5) mm s^{-1}]. Despite identical Fe^{II} donor sets and similar gross structural features (see above), the Mössbauer parameters of **2** [δ = 0.196(3) and ΔE_Q = 1.029(6) mm s^{-1}] differ significantly from those of **3**, possibly as a consequence of the dissymmetry (and possible additional strain) resulting from the presence of one ethylene and one propylene bridges in $L^{B'}$ (Chart 2) as compared to two propylene bridges in $L^{C'}$ (Chart 3).

Discussion and Theoretical Calculations

We focus this discussion on the different ligand forms in both the isolated and complexed states, and we first summarize the results evidenced by this work.

(1) The isolated ligands are in the dissymmetric (cyclic) isomeric forms L^A, L^B/L^{B*}, and L^C (Charts 1−3, respectively); i.e., the equilibria between the dissymmetric (cyclic) forms and isomeric acyclic Schiff bases mentioned by several authors (see Introduction) are totally shifted toward L^A, L^B/L^{B*}, and L^C in the case of the three condensation reactions under study here.

(2) *In solution*, the ligands coordinated to zinc are predominantly (or totally) either in the dissymmetric cyclic isomeric forms (L^A and L^{B°) or in the symmetric acyclic Schiff base isomeric form $L^{C'}$; i.e., while dissymmetric isomeric forms are essentially retained upon complexation of zinc with L^A and L^B/L^{B*}, the isomeric form L^C is shifted toward the Schiff base isomeric form $L^{C'}$ upon complexation of zinc.

In the solid state, the following exist:

(3) Regardless of the metal center (Fe^{II}, Ni^{II}, and Zn^{II}), the disymmetric isomeric form L^A of the ligand including one imidazolidine ring and one (short) ethylene bridge is stabilized through tetracoordination.

(4) Regardless of the metal center, the symmetric bis-Schiff base isomeric form $L^{C'}$ of the ligand including two (long) propylene bridges is stabilized through pentacoordination.

(5) The stabilized isomeric form of the ligand based on 3-[(2-aminoethyl)amino]propylamine (one ethylene bridge and one propylene bridge) depends on the metal center: iron(II) stabilizes the pentadentate bis-Schiff base isomeric form $L^{B'}$ in the LS complex **2**; nickel(II) stabilizes the tetradentate dissymmetric isomeric form L^B in the high-spin complex **5**; zinc(II) stabilizes the tetradentate disymmetric form L^{B° in complex **8** (L^{B° results from MeOH addition across the azomethine linkage of L^B).

(6) While the two NCS anions are cis-coordinated in **1**, **4**, **5**, and **8**, the 2-pyridine terminal fragments are cis-

(25) Nakamoto, K. *Infrared and Raman Spectra of Inorganic and Coordination Compounds*, 4th ed.; John Wiley & Sons: New York, 1986.
(26) (a) Tuchagues, J.-P.; Hendrickson, D. N. *Inorg. Chem.* **1983**, *22*, 2545−2552. (b) Mabad, B.; Cassoux, P.; Tuchagues, J.-P.; Hendrickson, D. N. *Inorg. Chem.* **1986**, *25*, 1420−1431. (c) Boinnard, D.; Bousseksou, A.; Dworkin, A.; Savariault, J. M.; Varret, F.; Tuchagues, J.-P. *Inorg. Chem.* **1994**, *33*, 271−281.
(27) Geary, W. J. *Coord. Chem. Rev.* **1971**, *7*, 81−122.
(28) Greenwood, N. N.; Gibb, T. C. *Mössbauer Spectroscopy*; Chapman and Hall: London, 1971.

coordinated in complexes including the ligands L^A (**1** and **4**) and L^B (**5**) and trans-coordinated in complex **8** including the ligand L^{B°.

These results suggest the following comments:

(a) Results 2, 4, and 5 above confirm that, in the presence of a metal center, equilibria allow the isomeric form that "better fits" the metal center to predominate. For example, (i) reaction of the cyclic isomers L^A and L^C (largely predominating in the isolated ligand) with Zn yields complexes in which the cyclic isomer either is retained (L^A, **7**) or is completely shifted toward the acyclic isomer ($L^{C'}$, **9**) both in solution and in the solid state; (ii) when the L^B/L^{B*} "mixture" is reacted with Ni^{II}, the $L^B \leftrightarrows L^{B*}$ equilibrium is totally shifted toward L^B and only complex **5** is obtained.

(b) Results 2 and 4 show, in addition, that when a ligand includes long enough bridges (here propylene) for allowing pentacoordination of the bis-Schiff base isomer ($L^{C'}$) to compete with tetracoordination of the disymmetric (hexahydropyrimidine) isomer (L^C), the gain in stability yielded by pentacoordination versus tetracoordination allows a complete shift of the $L^C \leftrightarrows L^{C'}$ equilibrium toward $L^{C'}$.

(c) Results 2 and 3, on the other hand, show that when a ligand does not include long enough bridges (here ethylene) for allowing pentacoordination of the bis-Schiff base isomer ($L^{A'}$), then tetracoordination of the dissymmetric (imidazolidine) isomer (L^A) is the only reaction that may occur and the only complexes obtained are of the $[M^{II}L(NCS)_2]$ type (complexes **1**, **4**, **5**, and **7** illustrate this situation).

(d) Result 5 illustrates the interesting case where the nature of the bridges (one ethylene and one propylene) yields an intermediate situation, such that, at variance with results 3 and 4, the template role of the metal center is prominent in shifting the ligand equilibria toward the isomeric form most appropriate to each specific cation. LS Fe^{2+} has a small enough ionic radius (75 pm)[24] to stabilize the pentadentate bis-Schiff base isomer $L^{B'}$ in the LS complex **2**. The ionic radius of Ni^{2+} (83 pm)[24] is probably too large for allowing pentacoordination of the bis-Schiff base isomer $L^{B'}$, and thus it stabilizes the tetradentate isomer L^B in complex **5**. The ionic radius of Zn^{2+} (88 pm)[24] is even larger: a mismatch of the tetradentate isomeric form L^B with Zn^{2+} coordinative requirements probably allows a nucleophilic attack of the C═N imine by the solvent (methanol), which results in MeOH addition across C═N. The gain in flexibility of L^{B° compared to L^B then allows complexation of the tetradentate dissymmetric form L^{B° to Zn^{2+} in complex **8**.

(e) For simplicity, the arguments mentioned in the above comments b−d rely essentially on size effects: however, the stereochemical preference of the complexed metal ion is also very important, although both types of effects may generally be hardly distinguished. This may be illustrated by considering **7** and **8**: while the "smaller" tetradentate ligand L^A including one ethylene bridge and one imidazolidine ring is tetracoordinated to Zn^{2+} in **7**, the "larger" tetradentate ligand L^B including one ethylene bridge and one hexahydropyrimidine ring does not yield a Zn^{2+} complex similar to **7**. It is then clear that size effects cannot explain why the same Zn^{2+} cation is chelated by L^A (**7**) but not by L^B. In this case, the stereochemical preference of Zn^{2+} allows L^A but not L^B to act as a tetradentate ligand.

(f) The acidity of the metal center does not seem to have a significant effect on the ligand equilibria: the splitting of the imidazolidine/hexahydropyrimidine ring with a gain in ligand denticity (from 4 to 5) is similarly achieved by such different Lewis acids as Fe^{2+} (**2**, $L^B \rightarrow L^{B'}$; **3**, $L^C \rightarrow L^{C'}$), Ni^{2+} (**6**, $L^C \rightarrow L^{C'}$), and Zn^{2+} (**9**, $L^C \rightarrow L^{C'}$). Thus, our results disagree with the following statement: "Weak Lewis acids (Fe^{2+}, Co^{2+}, and Cu^{2+}) are incapable (or only partly capable) of splitting the imidazolidine ring, whereas strong Lewis acids (Fe^{3+} and Zn^{2+}) can readily do so."[12a]

In the case (Zn) where qualitative information was gained suggesting that the ligand isomeric forms observed in solution are the same as those evidenced in the solid state, it may be assumed that these isomeric forms are thermodynamically favored. However, considering the absence of information about the species in solution for the Fe^{II} and Ni^{II} complexes and the qualitative nature of the information yielded by the solution studies for the Zn complexes, it was essential to independently evaluate the origin of the selective formation of complexes including different isomeric forms of the ligands depending on the metal center and on the ligand. This was then accomplished by investigating the relative stability of all possible isomeric complexes at the DFT level. Considering its particular interest, we have focused on the case of $L^B/L^{B*}/L^{B^\circ}$, where the role of the metal center is prominent in shifting the ligand equilibria toward the isomeric form most appropriate to each specific metal cation.

DFT Calculations. In principle, six isomers (Chart 5) may be formed upon complexation of a metal cation (M = Ni^{2+} and Zn^{2+}) with the ligand L^B/L^{B*}. In isomers **Ia** and **Ia′**, the pyridine rings of L^B/L^{B*} are trans to each other whereas the thiocyanate ligands are cis-coordinated. In isomers **IIa** and **IIa′**, the pyridine rings of L^B/L^{B*} as well as the thiocyanate anions are cis-coordinated. Finally, in isomers **IIIa** and **IIIa′**, the thiocyanate anions are trans to each other whereas the pyridine rings of the ligand are cis-coordinated. In the sole case of Zn^{2+}, the addition of methanol occurs on the C═N imine bond of the tetradentate ligand L^B/L^{B*} and, similarly to the case described above, six isomers **Ib**,**b′**−**IIIb**,**b′** may be considered: two of them (**Ib** and **Ib′**) are sketched at the bottom of Chart 5.

However, experimentally, by reaction of a metal salt with L^B/L^{B*}, depending on the metal center, only one isomer among the six possible ones is obtained. For Ni^{2+}, isomer **IIa** is obtained with a hexahydropyrimidine cycle and the pyridine rings of the ligand cis to each other, while in the case of Zn^{2+}, isomer **Ib** is obtained with an L^{B° hexahydropyrimidine cycle and the pyridine rings of the ligand trans to each other.

To understand the origin of the selective formation of one isomer among the six possible ones, the relative stabilities of isomers **Ia**,**a′**−**IIIa**,**a′**, on the one hand, and of isomers **Ib**,**b′**−**IIIb**,**b′**, on the other hand, were investigated at the DFT level. The structures of the various isomers were

Chart 5. Six Possible Isomers (**Ia**,**a′**−**IIIa**,**a′**) and Two (**Ib** and **Ib′**) among the Six Possible Isomers Resulting from Complexation of a Metal Center by the Ligands L^B/L^{B*} and $L^{B°}/L^{B°*}$, Respectively

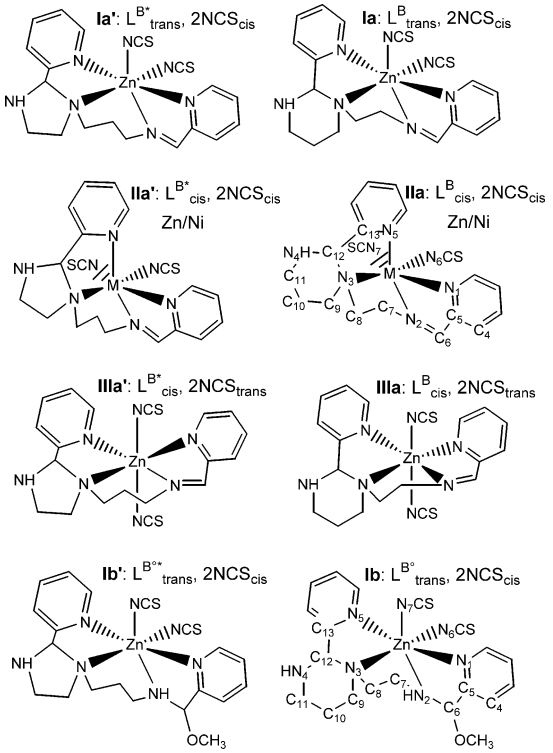

Table 2. Comparison of Experimental (X-ray Structure of Complex **5**) and Calculated (DFT for Ni^{2+} and Zn^{2+}) Selected Geometrical Data for Structure **IIa** (Distances, Å; Angles, deg)

	exptl Ni^{2+} (**5**)	calcd Ni^{2+}	calcd Zn^{2+}		exptl Ni^{2+} (**5**)	calcd Ni^{2+}	calcd Zn^{2+}
M−N1	**2.085**	**2.146**	**2.266**	N3−C12	1.511	1.497	1.493
N1−C5	1.358	1.352	1.347	C12−C13	1.507	1.518	1.520
C5−C4	1.381	1.392	1.393	**M−N5**	**2.114**	**2.137**	**2.342**
C5−C6	1.451	1.470	1.474	**M−N6**	**2.045**	**1.984**	**1.968**
N2−C6	1.268	1.275	1.272	**M−N7**	**2.070**	**2.038**	**2.038**
M−N2	**2.036**	**2.030**	**2.151**	py−py	93.5	99.1	96.7
N2−C7	1.437	1.442	1.441	N1−M−N2	78.1	77.1	73.3
C7−C8	1.504	1.527	1.529	N3−M−N5	76.9	77.6	71.7
N3−C8	1.626	1.482	1.478	S−C−N6	153.3	132.0	130.4
M−N3	**2.172**	**2.201**	**2.300**	S−C−N7	168.0	152.0	151.5

calculated at the B3PW91/6-31G* level. The influence of the nature of the transition metal was investigated for **IIa** and **IIa′** only. Ni complexes were considered in the triplet spin state. The envelope (chair) conformation observed experimentally for the imidazolidine (hexahydropyrimidine) ring was generally used in the calculations. Similarly, the alkyl chain conformation and C6 and N2 configurations observed experimentally were used in the **Ib**,**b′**−**IIIb**,**b′** calculations. In addition, the influence of the ring and/or alkyl chain conformation and C6 and N2 configurations was studied on a few examples.

The experimental and calculated structures **IIa** (M = Ni^{2+}) are compared in Table 2 through selected geometrical data. The agreement is very good, suggesting that the level of calculation is relevant to study this series of complexes. As expected, upon substitution of Ni^{2+} by Zn^{2+}, the metal−ligand bonds are lengthened, whereas the other bonds are little affected.

Table 3. Relative Energies (kcal mol^{-1}) of the **IIa**,**a′** Ni and **Ia**,**a′**−**IIIa**,**a′** Zn Isomers

compound	ΔE^a (kcal mol^{-1})	comment
IIa (Ni^{2+})	0.0	triplet spin state
IIa′ (Ni^{2+})	4.3	triplet spin state
IIa (Zn^{2+})	0.0	chair conformation of the C_4N_2 cycle
IIa (Zn^{2+})	6.4	boat conformation of the C_4N_2 cycle
IIa′ (Zn^{2+})	5.3	
Ia (Zn^{2+})	9.0	N2 decoordination
Ia′ (Zn^{2+})	7.9	M−N3 and M−N1 bonds are lengthened
IIIa (Zn^{2+})	7.8	M−N1 bond is lengthened
IIIa′ (Zn^{2+})	9.7	

[a] ∼1 kcal mol^{-1} accuracy allowed by calculations at the DFT level.

Table 4. Comparison of Experimental (X-ray Structure of Complex **8**) and Calculated (DFT for Zn^{2+}) Structure **Ib** (Distances, Å; Angles, deg)

	exptl Zn^{2+} (**8**)	calcd Zn^{2+}		exptl Zn^{2+} (**8**)	calcd Zn^{2+}
Zn−N1	2.184	2.201	N3−C12	1.493	1.482
N1−C5	1.335	1.338	C12−C13	1.496	1.513
C5−C4	1.386	1.392	Zn−N5	2.173	2.214
C5−C6	1.511	1.519	Zn−N6	2.075	1.969
N2−C6	1.443	1.456	Zn−N7	2.085	1.993
Zn−N2	2.221	2.356	py−py	170.0	163.5
N2−C7	1.458	1.462	N2−Zn−N3	80.0	74.2
C7−C8	1.510	1.524	N3−Zn−N5	75.8	71.7
N3−C8	1.483	1.467	S−C−N6	169.5	155.4
Zn−N3	2.238	2.446	S−C−N7	170.7	168.8

The relative stabilities of the various isomers **Ia**,**a′**−**IIIa**,**a′** are compared in Table 3 (M = Ni and Zn).

In agreement with the experimental results, **IIa** is the most stable isomer for M = Ni^{2+} and Zn^{2+} (Table 3). In the latter case, **IIa′** is more than 5 kcal mol^{-1} higher in energy than **IIa** while the other isomers are more than 8 kcal mol^{-1} higher in energy than **IIa**. This may explain why they are not observed experimentally.

The cis arrangement of N1 and N5 (pyridine donors) is the most favorable. By contrast, their trans arrangement appears to be very unfavorable. The strain resulting from the required coplanarity of N1 with the adjacent N2 (imine donor) is released by decoordination of N1 in the optimized structure of the *trans*-pyridine isomer **Ia**. Similarly, the trans arrangement of S−C−N6 and S−C−N7 also appears to be very unfavorable. M−N3 and M−N1 are lengthened by about 0.2 Å in the optimized structures **Ia′** and **IIIa** as compared to the corresponding bond length in the more stable isomer **IIa**.

Coordination of the L^B isomer (hexahydropyrimidine ring) appears to be generally more favorable than coordination of L^{B*} (imidazolidine ring) whatever the relative arrangement of donors (schematic structures in Chart 5). Structure **IIa** is significantly more stable than **IIa′** (ΔE = 5.3 kcal mol^{-1}).

(a) Relative Stabilities of the Isomers of $L^{B°}$ Resulting from the Addition of Methanol to L^B. The experimental and calculated structures **Ib** (M = Zn) are compared in Table 4 through selected geometrical data. Again, the agreement is very good, validating the level of calculation. The Zn−ligand bonds are slightly longer in the calculated structure as compared to the experimental structure.

The relative stabilities of the various isomers **Ib**,**b′**−**IIIb**,**b′** are compared in Table 5 for M = Zn^{2+}. As a result of

Table 5. Relative Energies (kcal mol^{-1}) of the Zn Isomers **Ib**,**b′**−**IIIb**,**b′**

compd	ΔE (kcal mol^{-1})	comment
Ib	0.0	
Ib′	12.3	M−N2 and M−N3 bonds are lengthened
IIb	9.7	boat conformation of the C_4N_2 cycle; N2 inversion
IIb′	12.7	N2 inversion
IIIb	11.3	Zn−N1 = 3.9 Å: decoordination of pyridine
IIIb′	16.8	
IIIb′	13.2	N2 inversion

methanol addition on N2 (imine), the relative stabilities of the Zn isomers are modified. In agreement with the experimental results, **Ib** is the most stable isomer. The other isomers are calculated to be more than 9 kcal mol^{-1} higher in energy.

In agreement with the experimental results, isomer **Ib** with $L^{B°}$ (hexahydropyrimidine cycle) and the pyridine rings of the ligand trans to each other is the most stable. The cis arrangement of N1 and N5 (pyridine donors) results in steric strain, which is released by decoordination of N1 upon geometry optimization of isomer **IIIb**.

Again, coordination of isomer $L^{B°}$ (hexahydropyrimidine ring) appears to be generally more favorable than coordination of $L^{B°*}$ (imidazolidine ring) whatever the relative arrangement of donors (structures in Chart 5). Structure **Ib** is significantly more stable than **Ib′** (ΔE = 12.3 kcal mol^{-1}).

(b) Influence of the Ring Conformations. At the B3PW91/6-31G* level of calculation, the boat conformation of the hexahydropyrimidine ring is less stable (ΔE = 7.7 kcal mol^{-1}) than the chair conformation experimentally observed and generally considered in our calculations. This energy difference is slightly reduced (ΔE = 6.38 kcal mol^{-1}) when the conformation of the six-membered ring is changed within **IIa** (Table 3). The envelope (chair) conformation observed experimentally for the imidazolidine (hexahydropyrimidine) ring was generally used in the previously described calculations because it is the most stable. For example, N2 inversion of the imidazolidine ring (**IIIb′**) requires a ∼3.6 kcal mol^{-1} increase in energy (Table 5). Complexes with other heterocyclic conformations or N2 inversion are 4−6 kcal mol^{-1} higher in energy than the ones described in Tables 3 and 5. These conformation changes are therefore not able to change the relative stabilities of the various isomers.

Conclusions

The condensation reaction between 2-pyridinecarboxaldehyde and diethylenetriamine, 3-[(2-aminoethyl)amino]-propylamine, or 3,3′-iminobis(propylamine) in a 2:1 molar ratio yields ligands that may be isolated exclusively in the dissymmetric (cyclic) isomeric forms L^A, L^B/L^{B*}, and L^C (Charts 1−3, respectively). In the absence of a metal center, we have shown, at variance with ref 11, that the formation of cyclic isomers is quantitative, although an intramolecular H bond cannot be established between the pyridine and imidazolidine (or hexahydropyrimidine) moieties. We have clarified which isomeric form, cyclic (hexahydropyrimidine or imidazolidine) or acyclic Schiff base, is initially formed: this implies different reaction pathways and mechanisms and had not previously been fully discussed and settled with undisputable arguments. On the basis of our experimental results and at variance with ref 12a, we have suggested a detailed mechanism that lends support to the formation of cyclic isomers *prior* to Schiff bases.

We have then clarified the respective roles of the ligand and metal center in yielding complexes with either the cyclic or acyclic isomer. Through a full combination of three different ligands and three different metal ions yielding nine complexes, we have clearly identified the ligand-related or metal-cation-related factors responsible for ring opening upon complexation, a task that had not been previously achieved. We have shown the prominent role of the ionic radius of the metal center: regardless of the metal, Fe^{2+}, Ni^{2+}, and Zn^{2+}, the ligand L^A including an imidazolidine ring [based on the $-N(CH_2)_2N-$ motif] chelates the metal center without opening its ring, yielding **1**, **4**, and **7**. In contrast, the hexahydropyrimidine ring of the ligand L^C [based on the $-N(CH_2)_3N-$ motif] is opened upon complexation regardless of the metal, Fe^{2+}, Ni^{2+}, and Zn^{2+}, yielding **3**, **6**, and **9**. These results prove the prominent role of the ligand [$-N(CH_2)_2N-$ vs $-N(CH_2)_3N-$ bridges]. In the case of the ligand L^B/L^{B*} based on the dissymmetric triamine, the opening of the ring upon complexation depends on the size of the metal cation: while LS Fe^{II} has a small enough ionic radius (75 pm) to stabilize the pentadentate Schiff base isomer $L^{B′}$ (ring opening), yielding **2**, the ionic radius of Ni^{II} (83 pm) is too large for allowing pentacoordination of the Schiff base isomer, and thus Ni^{II} stabilizes the tetradentate cyclic isomer, yielding **5**. These results prove that, provided an adequate ligand is chosen, the prominent role of the ionic radius (not the Lewis acidity[12a]) can be evidenced.

DFT calculations performed on the isomers sketched in Chart 5 allow one to show that isomerization, or methanol addition across the imine bond, of the tetradentate ligand depends on the relative stabilities of all possible isomeric complexes. This suggests that isomer selectivity is under thermodynamical rather than kinetic control. Among the possible isomers, **IIa** is the most stable whatever the metal center. In the presence of Zn, however, methanol addition occurs across the imine bond of L^B, thus converting it into a single C−N bond. The steric strain is then released by coordination of the N−pyridine rings trans to each other in the most stable isomer **Ib**.

Experimental Section

Physical Measurements. Microanalyses for C, H, N, and S were performed by the Microanalytical Laboratory of the Laboratoire de Chimie de Coordination in Toulouse, France, and the Service Central de Microanalyses du CNRS in Vernaison, France, for Fe, Ni, and Zn. 1D ^{1}H and ^{13}C NMR spectra were performed on an AC 250 FT spectrometer (Bruker). Chemical shifts are given in ppm relative to tetramethylsilane (^{1}H and ^{13}C) using $(CD_3)_2SO$ or CD_3CN as the solvent. Electrical conductivity measurements were carried out at room temperature on a CONSORT C832 digital

Table 6. Crystallographic Data and Refinement Parameters for Compounds **1**, **3**−**6**, and **8**

	1	**3**	**4**	**5**	**6**	**8**
formula	$C_{18}H_{19}N_7S_2Fe$	$C_{20}H_{22}N_7S_2Fe$	$C_{18}H_{19}N_7S_2Ni$	$C_{19}H_{21}N_7S_2Ni$	$C_{20}H_{23}N_7S_2Ni$	$C_{20}H_{27}N_7O_2S_2Zn$
formula weight	453.37	481.42	456.23	470.26	484.28	526.98
cryst syst	monoclinic	monoclinic	monoclinic	monoclinic	monoclinic	monoclinic
space group	*Cc*	$P2_1/m$	*Cc*	$P2_1/c$	$P2_1/m$	$P2_1/n$
a, Å	13.5853(17)	8.0433(9)	13.726(3)	11.1512(16)	8.0178(16)	8.7588(8)
b, Å	13.1522(10)	9.5361(7)	13.221(3)	13.2683(16)	9.6784(19)	13.8619(8)
c, Å	13.0116(15)	14.4027(15)	13.107(3)	14.217(2)	14.546(3)	20.8629(13)
β, deg	112.213(13)	101.851(13)	112.32(3)	92.834(12)	101.21(3)	99.136(6)
V, Å^3	2152.3(4)	1081.16(18)	2200.4(8)	2101.0(5)	1107.2(4)	2500.9(3)
Z	4	2	4	4	2	4
T, K	180	180	180	180	180	180
ρ(calcd), Mg m^{-3}	1.399	1.479	1.377	1.487	1.453	1.400
λ, Å	0.71073	0.71073	0.71073	0.71073	0.71073	0.71073
μ(Mo Kα), mm^{-1}	0.913	0.913	1.089	1.143	1.087	1.179
R [$I > 2\sigma(I)$][a]	0.0244	0.0982	0.0386	0.0496	0.0783	0.0671
wR[b]	0.0683	0.2162	0.1004	0.0967	0.1932	0.1781

[a] $R = \sum||F_o| - |F_c||/\sum|F_o|$. [b] $wR = [\sum w(|F_o^2| - |F_c^2|)^2/\sum w|F_o^2|^2]^{1/2}$.

conductometer [cell constant (K) = L/S = 0.117, alternating electrical current] in ca. 10^{-3} M acetonitrile solutions. Infrared spectra (4000−400 cm^{-1}) were recorded as KBr disks on a Perkin-Elmer Spectrum GX FT-IR spectrometer. Magnetic susceptibility data were collected on powdered microcrystalline samples with a Faraday balance. Data were corrected with the standard procedure for the contribution of the sample holder and diamagnetism of the sample. Mössbauer measurements were recorded on a constant-acceleration conventional spectrometer with a 50 mCi source of ^{57}Co (Rh matrix). The absorber was a powdered sample enclosed in a 20-mm-diameter cylindrical plastic sample holder, the size of which had been determined to optimize the absorption. Spectra were obtained in the 80−300 K range, by using an Oxford MD 306 cryostat, with the thermal scanning being monitored by an Oxford ITC4 servocontrol device (±0.1 K accuracy). A least-squares computer program was used to fit the Mössbauer parameters and determine their standard deviations of statistical origin (given in parentheses).[29] Isomer shift values (δ) are relative to iron foil at 293 K.

Crystal Structure Determination of Compounds 1, 3−6, and 8. The X-ray data for compounds **1** and **3** were collected at 180 K on a Stoe Imaging Plate Diffractometer System (IPDS) equipped with an Oxford Cryosystems cooler device using a graphite monochromator (λ = 0.710 73 Å). Data were collected[30] using φ rotation movement with the crystal-to-detector distance equal to 70 mm (φ = 0.0−250° and $\Delta\varphi$ = 1.5° for **1** and φ = 0.0−200° and $\Delta\varphi$ = 2.0° for **3**). Crystallographic measurements for **4**−**6** and **8** were carried out at 180 K with an Oxford Diffraction XCALIBUR CCD diffractometer using graphite-monochromated Mo Kα radiation. The crystals were placed 60 mm from the CCD detector. More than the hemisphere of reciprocal space was covered by a combination of four sets of exposures; each set had a different φ angle (0, 90, 180, and 270°). Coverage of the unique set is 99.8% complete up to 2θ = 52°. The unit cell determination and data integration were carried out using the CrysAlis package of Oxford Diffraction.[31] Intensity data were corrected for Lorentz and polarization effects.

All structures were solved by direct methods using SHELXS-97[32] and refined by full-matrix least squares on F_o^2 with SHELXL-97[33] with anisotropic displacement parameters for non-hydrogen atoms. All hydrogen atoms attached to carbon were introduced in idealized positions (d_{CH} = 0.96 Å) using the riding model with their isotropic displacement parameters fixed at 120% of their riding atom. In the two isostructural compounds **1** and **4**, the sulfur atom of one NCS^- anion presented large thermal ellipsoids and disordered models were applied in order to better fit the electron density. The same approach, in combination with the available tools (PART, DFIX, and SADI) of SHELXL97, was used for complexes **3** and **6** because of the disorder in the central part of the $L^{C'}$ pentadentate ligand: Fe, Ni, both coordinated and out-of-sphere thiocyanate anions, and N1, N3, N5, and C3 atoms of the Schiff base ligand reside in special positions on the C_s glide plane. All other atoms in the structure are disordered over two symmetrically related positions around the C_s plane. Scattering factors were taken from the standard compilation.[34] The molecular plots were obtained using the ZORTEP program.[35] Relevant crystallographic data together with refinement details are summarized in Table 6.

Computational Details for DFT Calculations. Geometries of the various isomers were constructed from experimental structures and were fully optimized at the B3PW91/6-31G* level using Gaussian98[36] or Gaussian03.[37] Vibrational analysis was performed at the same level in order to check that a minimum was obtained on the potential energy surface.

Materials. All reagents and solvents used in this study are commercially available (Aldrich) and were used without further purification. All syntheses involving Fe^{II} were carried out under a

(29) Lagarec, K. *Recoil, Mössbauer Analysis Software for Windows*. http://www.physics.uottawa.ca/~recoil.

(30) STOE, *IPDS Manual*, version 2.93; Stoe & Cie: Darmstadt, Germany, 1997.

(31) *CrysAlis RED*, version 1.170.32; Oxford Diffraction Ltd.: Oxford, U.K., 2003.

(32) Sheldrick, G. M. *SHELXS-97, Program for Crystal Structure Solution*; University of Göttingen: Göttingen, Germany, 1990.

(33) Sheldrick, G. M. *SHELXL-97, Program for the refinement of crystal structures from diffraction data*; University of Göttingen: Göttingen, Germany, 1997.

(34) *International Tables for Crystallography*; Kluwer Academic Publishers: Dordrecht, The Netherlands, 1992; Vol. C.

(35) Zsolnai, L.; Pritzkow, H.; Huttner, G. *ZORTEP, ORTEP for PC, Program for Molecular Graphics*; University of Heidelberg: Heidelberg, Germany, 1996.

(36) Frisch, M. J.; Trucks, G. W.; Schlegel, H. B.; Scuseria, G. E.; Robb, M. A.; Cheeseman, J. R.; Zakrzewski, V. G.; Montgomery, J. A., Jr.; Stratmann, R. E.; Burant, J. C.; Dapprich, S.; Millam, J. M.; Daniels, A. D.; Kudin, K. N.; Strain, M. C.; Farkas, O.; Tomasi, J.; Barone, V.; Cossi, M.; Cammi, R.; Mennucci, B.; Pomelli, C.; Adamo, C.; Clifford, S.; Ochterski, J.; Petersson, G. A.; Ayala, P. Y.; Cui, Q.; Morokuma, K.; Malick, D. K.; Rabuck, A. D.; Raghavachari, K.; Foresman, J. B.; Cioslowski, J.; Ortiz, J. V.; Baboul, A. G.; Stefanov, B. B.; Liu, G.; Liashenko, A.; Piskorz, P.; Komaromi, I.; Gomperts, R.; Martin, R. L.; Fox, D. J.; Keith, T.; Al-Laham, M. A.; Peng, C. Y.; Nanayakkara, A.; Gonzalez, C.; Challacombe, M.; Gill, P. M. W.; Johnson, B.; Chen, W.; Wong, M. W.; Andres, J. L.; Gonzalez, C.; Head-Gordon, M.; Replogle, E. S.; Pople, J. A. *Gaussian 98*, revision A.7; Gaussian, Inc.: Pittsburgh, PA, 1998.

purified nitrogen atmosphere in an inert-atmosphere box (Vacuum Atmospheres HE 43-2) equipped with a dry train (Jahan EVAC 7).

Preparation of the Ligands. A total of 2 equiv of pyridine-2-carboxaldehyde (0.214 g, 2×10^{-3} mol) and 1 equiv of diethylenetriamine (0.104 g, 10^{-3} mol) for L^A, 1 equiv of 3-[(2-aminoethyl)amino]propylamine (0.117 g, 10^{-3} mol) for L^B/L^{B*}, and 1 equiv of 3,3′-iminobis(propylamine) (0.132 g, 10^{-3} mol) for L^C were stirred for 2 h in 20 mL of CH_2Cl_2 at room temperature. Slow evaporation of the solvent yielded a light-brown oil for each ligand [yield: 0.28 g (91%), 0.31 g (95%), 0.32 g (92%) for L^A, L^B/L^{B*}, and L^C, respectively]. The ligands were characterized by ^{1}H and ^{13}C NMR in DMSO-d_6 (δ, ppm; s, singlet; d, doublet; t, triplet; dt = doublet of triplets; m, multiplet; b, broad).

L^A: ^{1}H NMR (250 MHz) δ 8.62 (d, $J = 6$ Hz, H_{14}, 1H), 8.46 (d, $J = 4.5$ Hz, H_4, 1H), 8.25 (s, H_6, 1H), 7.85 (d, $J = 4.5$ Hz, $H_1 + H_{17}$, 1H + 1H), 7.68 (t, $J = 6$ and 1.5 Hz, H_2, 1H), 7.50 (t, $J = 7$ Hz, H_{15}, 1H), 7.44 (t, $J = 6$ Hz, H_{16}, 1H), 7.27 (td, $J = 5$ and 1.5 Hz, H_3, 1H), 4.21 (s, H_{12}, 1H), 3.38 (b, H_{11}, 1H), 2.60−3.7 (m, H_7, H_8, H_9, and H_{10}, 2H + 2H + 2H + 2H); ^{13}C NMR (63 MHz) δ 162.2 (C_6), 161.2 (C_{13}), 154.2 (C_5), 149.4 (C_{17}), 148.4 (C_1), 136.9 (C_3), 136.5 (C_{15}), 125.1 (C_4), 123.0 (C_{14}), 122.0 (C_{16}), 120.3 (C_2), 83.4 (C_{12}), 59.7 (C_7), 53.1 ($C_8 + C_9$), 44.7 (C_{10}).

L^B/L^{B*}: ^{1}H NMR (250 MHz) δ 8.61 (d, $J = 5$ Hz, H_{15} and H_{15}*, 1H + 1H), 8.46 (d, $J = 5$ Hz, H_4*, 1H), 8.41 (d, $J = 5$ Hz, H_4, 1H), 8.19 (s, H_6 and H_6*, 1H + 1H), 7.83−7.80 (m, H_1 and H_{18}, H_1*, and H_{18}*, 1H + 1H + 1H + 1H), 7.70−7.69 (m, H_2 and H_2*, 1H + 1H), 7.49−7.44 (m, H_{17}, H_{17}*, H_{16}, and H_{16}*, 1H + 1H + 1H + 1H), 7.28 (t, H_3*, 1H), 7.20 (t, H_3, 1H), 4.11 (s, H_{13} and H_{13}*, 1H + 1H), 3.29 (b, H_{12} and H_{12}*, 1H + 1H), 2.33−3.2 (m, H_7, H_8, H_9, H_{10}, and H_{11}; H_7*, H_8*, H_9*, H_{10}*, and H_{11}*, 2H + 2H + 2H + 2H + 2H + 2H + 2H + 2H + 2H + 2H); ^{13}C NMR (63 MHz) δ 162.2−161.6 (C_6 and C_6*), 161.3−160.8 (C_{14} and C_{14}*), 154.0 (C_5 and C_5*), 149.3−149.2 (C_{18} and C_{18}*), 148.3−148.2 (C^1 and C_1*), 136.6−136.4 (C_3 and C_{17}; C_3* and C_{17}*), 125−124.9 (C_4 and C_4*), 122.9−122.8 (C15 and C_{15}*), 122.1−121.7 (C_2 and C_2*), 120.2 (C_{16} and C_{16}*), 83.6 (C_{13}*), 81.5 (C_{13}), 57.9−57.8 (C_7 and C_7*), 53.1−52.7, 52.2−50.1 (C_8*; C_9 and C_9*; C_{10}*), 44.7−44.5 (C_{11} and C_{11}*), 29.5 (C10), 26.1 (C8).

NB: Evaluation of the 40:60 L^B/L^{B*} ratio based on the relative integrations resulting from the distinguishable signals at δ 8.46 (H_4*, int = 0.7) and 8.41 (H_4, int = 0.3) and at δ 7.28 (H_3*, int = 0.7) and 7.20 (H_3, int = 0.5).

L^C: ^{1}H NMR (250 MHz) δ 8.61 (d, $J = 5.5$ Hz, H_{16}, 1H), 8.41 (d, $J = 5.5$ Hz, H_4, 1H), 8.19 (s, H_6, 1H), 7.82 (td, $J = 7.5$ and 1.5 Hz, H_2, 1H), 7.72 (d, $J = 7.5$ Hz, H_1 or H_{19}, 1H), 7.61 (td, $J = 7.5$ and 1.5 Hz, H_{17}, 1H), 7.42 (d, $J = 5.5$ Hz, H_{18}, 1H + t (nonresolved), H_{19} or H_1, 1H), 7.18 (t, $J = 5.5$ Hz, H_3, 1H), 4.00 (s, H_{14}, 1H), 3.41 (b, H_{13}, 1H), 1.50−3.50 (m, H_7, H_8, H_9, H_{10}, H_{11}, and H_{12}, 2H + 2H + 2H + 2H); ^{13}C NMR (63 MHz) δ 161.5 (C_6), 160.8 (C_{15}), 154.0 (C_5), 149.1 (C_{19}), 148.3 (C_1), 136.6 (C_3), 136.3 (C_{17}), 124.9 (C_4), 122.6 (C_{16}), 121.8 (C_{18}), 120.2 (C_2), 82.0 (C_{14}), 57.9 (C_7), 51.6 (C_{10}), 50.2 (C_9), 44.0 (C_{12}), 27.0 (C_{11}), 26.3 (C_8).

$M(NCS)_2 \cdot x$MeOH (M = Fe, Ni, and Zn). $M(ClO_4)_2 \cdot xH_2O$ (10^{-3} mol, 1 equiv; M = Fe, Ni, and Zn) was reacted with potassium thiocyanate (0.195 g, 2×10^{-3} mol) in 10 mL of MeOH following a procedure adapted from the preparation of $Fe(py)_4(NCS)_2$.[38] After removal of potassium perchlorate through filtration, the freshly prepared $M(NCS)_2 \cdot x$MeOH was used immediately for the preparation of complexes **1**−**9**.

Caution! *Perchlorate salts and complexes are potentially explosive and should be handled in small quantities and with much care.*

Metal Complexes. A methanolic solution (10 mL, 10^{-3} mol) of $M(NCS)_2 \cdot x$MeOH (M = Fe^{II}, Ni^{II}, and Zn^{II}) was slowly added to the methanolic solution (10 mL, 10^{-3} mol) of the ligand. The resulting reaction mixtures (Fe^{II}, dark-blue solution; Ni^{II}, red solution; Zn^{II}, pale-yellow solution) were stirred for 30 min.

$[FeL^A(NCS)_2]$ (1). Slow evaporation (over 1 month) of the reaction mixture yielded dark-blue crystals suitable for X-ray analysis (0.15 g, 33%). Elem anal. Calcd (%) for $FeC_{18}H_{19}N_7S_2$ (453 g mol^{-1}): C, 47.69; H, 4.22; N, 21.53; S, 14.15; Fe, 12.32. Found:[39] C, 47.05; H, 4.20; N, 20.26; S, 14.01; Fe, 11.52. Molar conductivity: $\Lambda_M = 75$ S cm^2 mol^{-1}. μ_B: ~0 μ_B (293 K). Mössbauer spectroscopy (δ, ΔE_Q, mm s^{-1}): 80 K, $\delta = 0.389(2)$, $\Delta E_Q = 0.740(3)$; 293 K, $\delta = 0.313(2)$, $\Delta E_Q = 0.730(4)$.

$[FeL^{B'}(NCS)](NCS)$ (2). A dark-blue microcrystalline powder was obtained upon slow evaporation of the reaction mixture (0.19 g, 41%). Elem anal. Calcd (%) for $FeC_{19}H_{21}N_7S_2$ (467 g mol^{-1}): C, 48.83; H, 4.53; N, 20.98; S, 13.72; Fe, 11.95. Found:[39] C, 48.43; H, 4.04; N, 20.70; S, 13.92; Fe, 11.16. Molar conductivity: $\Lambda_M = 138$ S cm^2 mol^{-1}. μ_B: ~0 μ_B (293 K). Mössbauer spectroscopy (δ, ΔE_Q, mm s^{-1}): 293 K, $\delta = 0.196(3)$, $\Delta E_Q = 1.029(6)$.

$[FeL^{C'}(NCS)](NCS)$ (3). Dark-blue crystals suitable for X-ray analysis were obtained upon slow evaporation of the reaction mixture (0.30 g, 62%). Elem anal. Calcd (%) for $FeC_{20}H_{23}N_7S_2$ (481 g mol^{-1}): C, 48.90; H, 4.82; N, 20.37; S, 13.32; Fe, 11.60. Found:[39] C, 49.41; H, 4.42; N, 19.96; S, 13.22; Fe, 11.05. Molar conductivity: $\Lambda_M = 123$ S cm^2 mol^{-1}. μ_B: ~0 μ_B (293 K). Mössbauer spectroscopy (δ, ΔE_Q, mm s^{-1}): 293 K, $\delta = 0.268(3)$, $\Delta E_Q = 0.838(5)$.

$[NiL^A(NCS)_2]$ (4). After 2 days, red crystals suitable for X-ray analysis were obtained upon slow evaporation of the reaction mixture (0.10 g, 22%). Elem anal. Calcd (%) for $NiC_{18}H_{19}N_7S_2$ (456 g mol^{-1}): C, 47.39; H, 4.20; N, 21.49; S, 14.05; Ni, 12.87. Found: C, 47.04; H, 3.69; N, 20.93; S, 13.69; Ni, 12.38. Molar conductivity: $\Lambda_M = 66$ S cm^2 mol^{-1}. μ_B: ~3 μ_B (293 K).

$[NiL^B(NCS)_2]$ (5). Red-brown crystals suitable for X-ray analysis were obtained upon slow evaporation of the reaction mixture (0.13 g, 28%). Elem anal. Calcd (%) for $NiC_{19}H_{21}N_7S_2$ (470 g mol^{-1}): C, 48.53; H, 4.50; N, 20.85; S, 13.64; Ni, 12.49. Found: C, 48.48; H, 3.95; N, 20.60; S, 13.51; Ni, 12.13. Molar conductivity: $\Lambda_M = 69$ S cm^2 mol^{-1}. μ_B: ~3.2 μ_B (293 K).

(37) Frisch, M. J.; Trucks, G. W.; Schlegel, H. B.; Scuseria, G. E.; Robb, M. A.; Cheeseman, J. R.; Montgomery, J. A., Jr.; Vreven, T.; Kudin, K. N.; Burant, J. C.; Millam, J. M.; Iyengar, S. S.; Tomasi, J.; Barone, V.; Mennucci, B.; Cossi, M.; Scalmani, G.; Rega, N.; Petersson, G. A.; Nakatsuji, H.; Hada, M.; Ehara, M.; Toyota, K.; Fukuda, R.; Hasegawa, J.; Ishida, M.; Nakajima, T.; Honda, Y.; Kitao, O.; Nakai, H.; Klene, M.; Li, X.; Knox, J. E.; Hratchian, H. P.; Cross, J. B.; Adamo, C.; Jaramillo, J.; Gomperts, R.; Stratmann, R. E.; Yazyev, O.; Austin, A. J.; Cammi, R.; Pomelli, C.; Ochterski, J. W.; Ayala, P. Y.; Morokuma, K.; Voth, G. A.; Salvador, P.; Dannenberg, J. J.; Zakrzewski, V. G.; Dapprich, S.; Daniels, A. D.; Strain, M. C.; Farkas, O.; Malick, D. K.; Rabuck, A. D.; Raghavachari, K.; Foresman, J. B.; Ortiz, J. V.; Cui, Q.; Baboul, A. G.; Clifford, S.; Cioslowski, J.; Stefanov, B. B.; Liu, G.; Liashenko, A.; Piskorz, P.; Komaromi, I.; Martin, R. L.; Fox, D. J.; Keith, T.; Al-Laham, M. A.; Peng, C. Y.; Nanayakkara, A.; Challacombe, M.; Gill, P. M. W.; Johnson, B.; Chen, W.; Wong, M. W.; Gonzalez, C.; Pople, J. A. *Gaussian 03*, revision B.03; Gaussian, Inc.: Pittsburgh, PA, 2003.

(38) Erikson, N. E.; Sutin, N. *Inorg. Chem.* **1966**, *5*, 1834−1835.

(39) We suspect the poor analytical results obtained for compounds **1**−**3** to originate from the high reactivity of Fe^{II} with dioxygen. Indeed, the Mössbauer spectra of **1**−**3** measured on ground crystals show a single quadrupole doublet characteristic of LS Fe^{II} without any trace of other Fe species.

[NiL$^{C'}$(NCS)](NCS) (6). Red crystals suitable for X-ray analysis were obtained upon slow evaporation of the reaction mixture (0.11 g, 23%). Elem anal. Calcd (%) for $NiC_{20}H_{23}N_7S_2$ (484 g mol^{-1}): C, 49.60; H, 4.79; N, 20.25; S, 13.24; Ni, 12.20. Found: C, 49.27; H, 4.19; N, 19.82; S, 13.02; Ni, 11.98. Molar conductivity: Λ_M = 126 S cm^2 mol^{-1}. μ_B: ~2.9 μ_B (293 K).

[ZnL^{A}(NCS)$_2$] (7). Colorless crystals suitable for X-ray analysis were obtained upon slow evaporation of the reaction mixture for 1 week (0.40 g, 87%). Elem anal. Calcd (%) for $ZnC_{18}H_{19}N_7S_2$ (463 g mol^{-1}): C, 46.71; H, 4.14; N, 21.18; S, 13.85; Zn, 14.12. Found: C, 46.43; H, 3.79; N, 20.75; S, 13.52; Zn, 13.87. Molar conductivity: Λ_M = 123 S cm^2 mol^{-1}.

[ZnL$^{B'}$(NCS)$_2$]·H$_2$O (8). Colorless crystals suitable for X-ray analysis were obtained upon slow evaporation of the reaction mixture (0.39 g, 70%). Elem anal. Calcd (%) for $ZnC_{20}H_{27}N_7S_2O_2$ (509 g mol^{-1}): C, 47.19; H, 4.95; N, 19.26; S, 12.17; Zn, 12.41. Found: C, 47.17; H, 4.54; N, 19.16; S, 12.32; Zn, 12.62. Molar conductivity: Λ_M = 128 S cm^2 mol^{-1}.

[ZnL$^{C'}$(NCS)](NCS) (9). White microcrystals were obtained upon slow evaporation of the reaction mixture (0.12 g, 25%). Elem anal. Calcd (%) for $ZnC_{20}H_{23}N_7S_2$ (491 g mol^{-1}): C, 48.93; H, 4.72; N, 19.97; S, 13.06; Zn, 13.32. Found: C, 49.02; H, 4.37; N, 19.82; S, 12.83; Zn, 13.11. Molar conductivity: Λ_M = 190 S cm^2 mol^{-1}.

Acknowledgment. We thank Dr. J. P. Costes, Prof. R. Chauvin, Dr. C. Denier, and Dr. A. Suarez for helpful discussions, A. Sournia-Saquet for conductivity measurements, and J. F. Meunier for magnetic measurements. The authors also thank CALMIP (Calcul Intensif en Midi-Pyrénées, Toulouse, France), CINES (Centre Informatique National de l'Enseignement Supérieur, Montpellier, France), and IDRIS (Institut du Développement et des Ressources en Informatique Scientifique) for computing facilities and P. Arnaud for computational assistance.

Supporting Information Available: X-ray crystallographic files in CIF format for compounds **1**, **3**−**6**, and **8**. Calculated structures: atomic coordinates and total energy of calculated structures **Ia**,**a′**−**IIIa**,**a′**, **Ib**,**b′**−**IIIb**,**b′** (M = Zn), and **IIa**,**a′** (M = Ni). This material is available free of charge via the Internet at http://pubs.acs.org.

IC050791B